Characterizing Quantum Signal Processing Under Realistic Noise

Shivane Dadi[1] Dhruv Patel[1] Grecia Castelazo[1] Murphy Niu[1]

[1]University of California, Santa Barbara

Abstract

Quantum Signal Processing (QSP) is a powerful framework that enables the implementation of non-unitary operations on quantum states by embedding target functions within unitary transformations. **The problem:** Hardware imperfections perturb phase rotations distorting the realized polynomial. We analyze the effect of different realistic noise models in the QSP protocol.

Background: Quantum Signal Processing

Quantum Signal Processing (QSP) implements polynomial transformations of a scalar $x \in [-1, 1]$ as a product of phase rotations interleaved with a signal operator:

$$a(x) = \langle 0|U(x, \Phi)|0\rangle \tag{1}$$

$$U(x, \Phi) = e^{i\phi_0 Z} \prod_{j=1}^{d} e^{i \arccos(x) X} e^{i\phi_j Z} \tag{2}$$

where $\Phi = (\phi_0, \ldots, \phi_d)$ are real-valued **phase factors** computed through factoring methods such as Prony, Newton, and NLFT. [1, 4, 5]

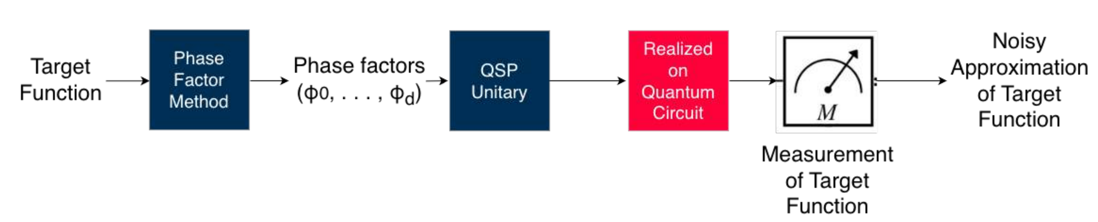

Example: Stochastic phase noise ($\sigma = 0.01$), error is concentrated at domain boundaries.

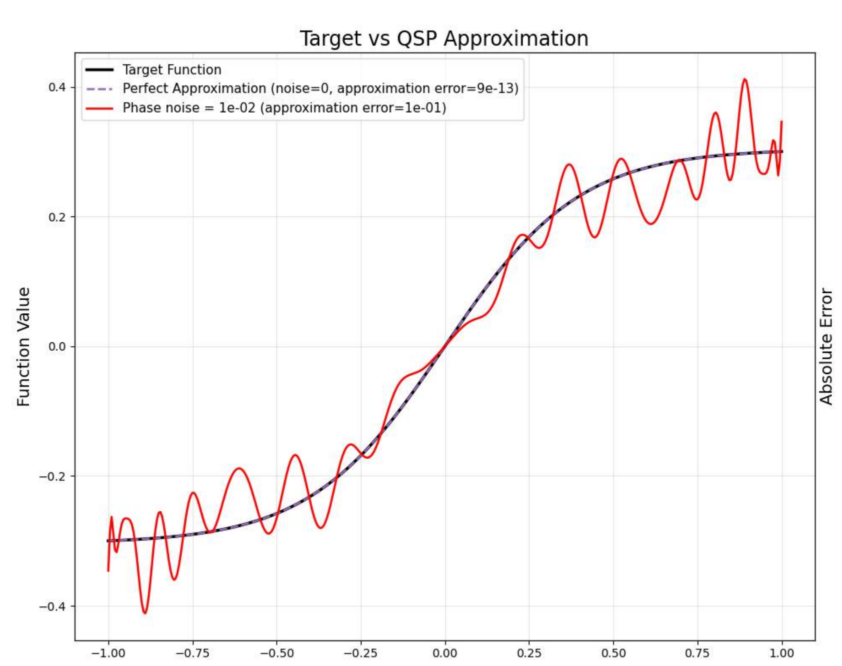

Approach

- Decompose realistic noise as unitary perturbations of QSP phase factors
- Derive first-order analytic predictions for each noise regime
- Benchmark and validate across phase-factor methods: Prony, Newton, NLFT

Coherent Noise Models

Additive Over/Under Rotation $\phi_j \mapsto \phi_j + \varepsilon$

First-order bound

$$|a_\varepsilon(x) - a(x)| \le (d+1)|\varepsilon| \tag{3}$$

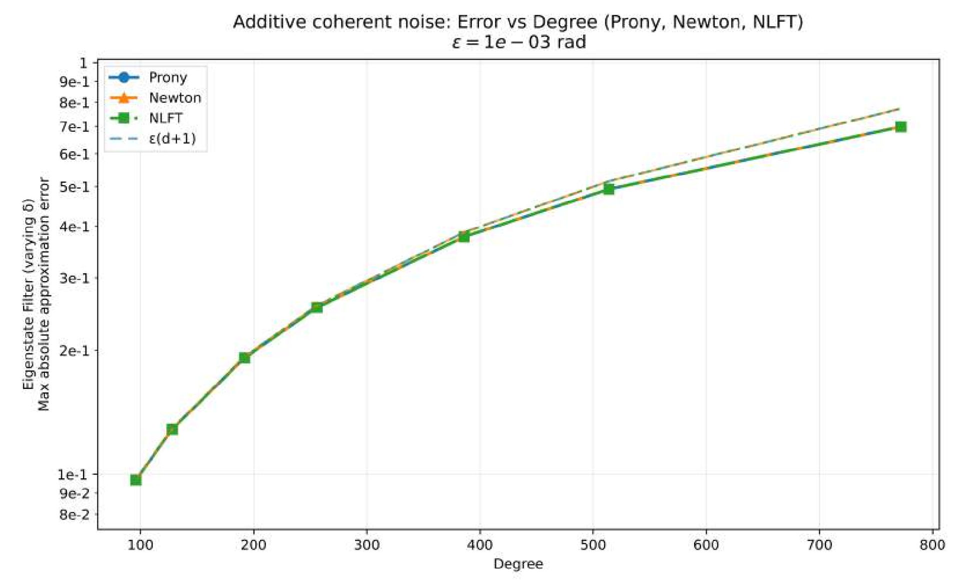

Multiplicative Over/Under Rotation: $\phi_j \mapsto \phi_j(1+\varepsilon)$ [2]

First-order prediction

$$|a_\varepsilon(x) - a(x)| \approx |\varepsilon| \cdot |\mathrm{Re}\, S(x)| \tag{4}$$

where $S(x) = \Sigma_j\, \phi_j P_j(x)$ and $P_j(x) = \langle 0|U_0^{(j)}|0\rangle$ is the $(0,0)$ entry with $\phi_j \to \phi_j + \pi/2$.

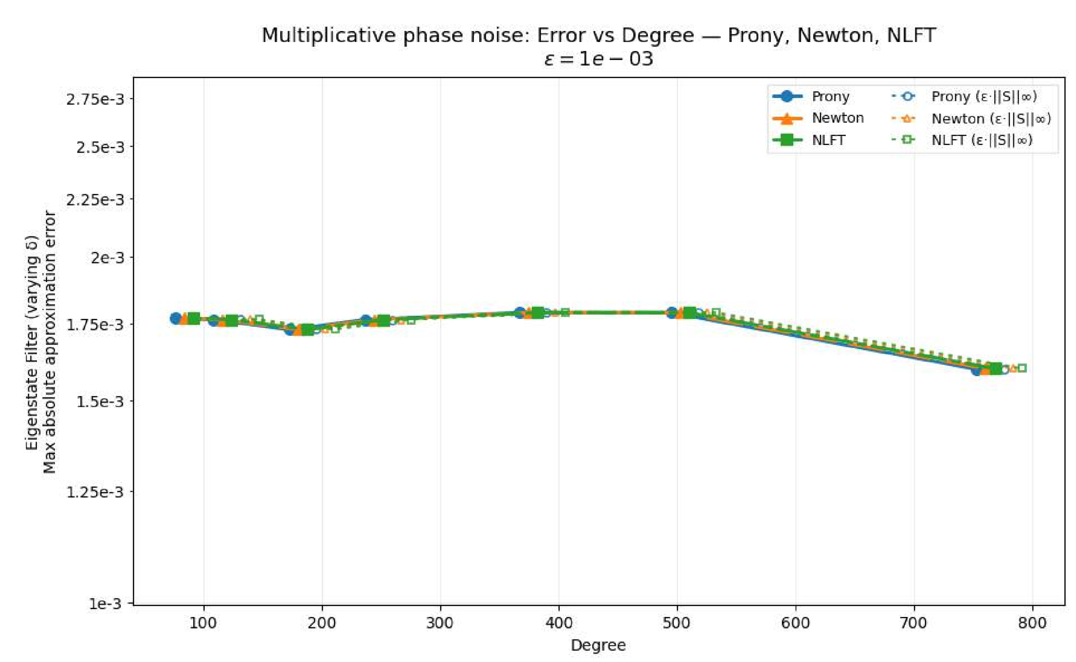

Figure 1. Multiplicative coherent error remains bounded as d grows

Stochastic Noise Models

Additive Stochastic $\phi_j \mapsto \phi_j + \varepsilon_j, \varepsilon_j \sim \mathcal{N}(0, \sigma^2)$ [3]

First-order bound

$$\sqrt{\mathbb{E}_\varepsilon |a_\varepsilon(x) - a(x)|^2} \lesssim \sigma\sqrt{d+1} \tag{5}$$

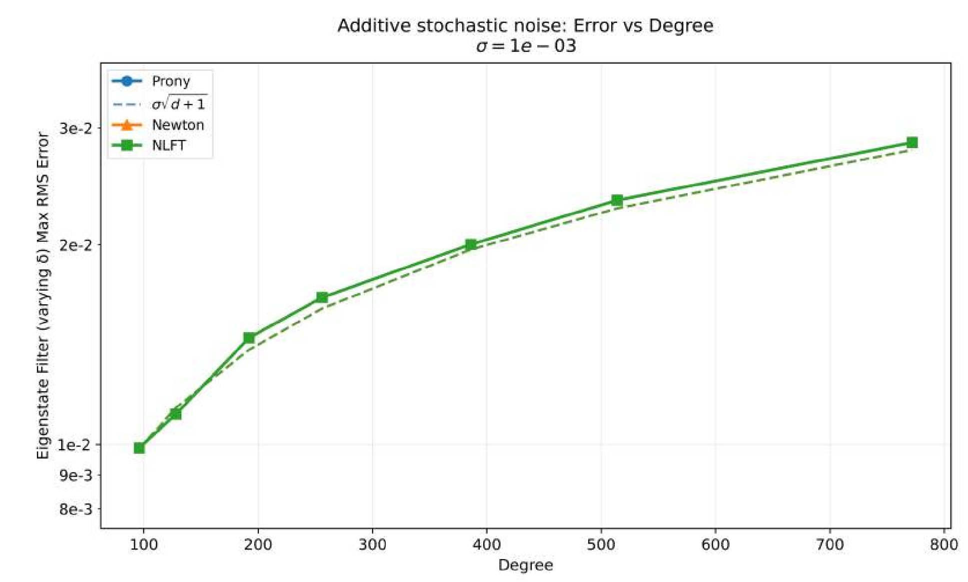

Figure 2. All methods collapse; error grows $\sim \sqrt{d}$.

Multiplicative Stochastic: $\phi_j \mapsto \phi_j(1+\varepsilon_j), \varepsilon_j \sim \mathcal{N}(0, \sigma^2)$

First-order bound

$$\sqrt{\mathbb{E}_\varepsilon |a_\varepsilon(x) - a(x)|^2} \lesssim \sigma\|\Phi\|_2 \tag{6}$$

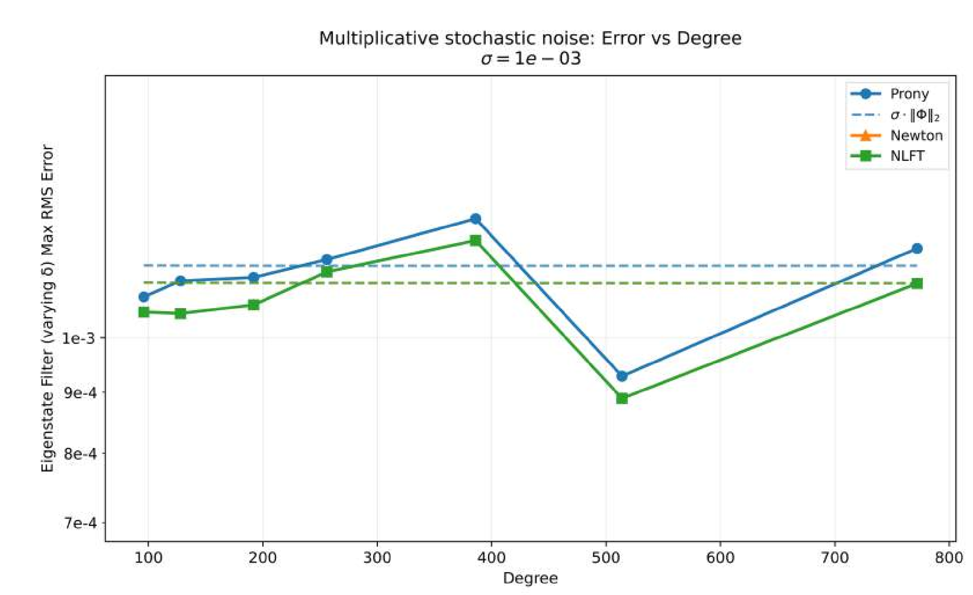

Figure 3. $\sigma\|\Phi\|_2$ tracks error to finite sampling accuracy

Cross-Function Validation at $d \approx 800$ ($\varepsilon = \sigma = 10^{-3}$)

Target Function	d	Clean Error	Add. Coh. $(d+1)\lvert\varepsilon\rvert$	Mult. Coh. $\lvert\varepsilon\rvert\lvert\mathrm{Re}\,S(x)\rvert$	Add. Stoch. $\sigma\sqrt{d+1}$	Mult. Stoch. $\sigma\|\Phi\|_2$
Eigenstate Filter	772	2.4×10^{-13}	6.98×10^{-1}	1.60×10^{-3}	6.14×10^{-2}	7.99×10^{-4}
Hamiltonian Sim	782	1.8×10^{-12}	6.09×10^{-1}	1.79×10^{-3}	5.99×10^{-2}	1.20×10^{-3}
Matrix Inversion	807	8.8×10^{-14}	7.25×10^{-1}	1.78×10^{-3}	6.40×10^{-2}	9.51×10^{-4}
Fermi-Dirac	791	5.8×10^{-12}	5.90×10^{-1}	1.79×10^{-3}	6.09×10^{-2}	1.15×10^{-3}

Empirical max-error across $x \in [-1, 1]$, shown for Newton; Prony and NLFT agree to within Monte Carlo precision. First-order analytical predictions (header) match observation across all four target families.

Results

Structural progression. Each noise model has a distinct first-order controlling quantity.

	Coherent	Stochastic RMS
Add.	$(d+1)\lvert\varepsilon\rvert$	$\sigma\sqrt{d+1}$
Mult.	$\lvert\varepsilon\rvert\,\lvert\mathrm{Re}\,S(x)\rvert$	$\sigma\|\Phi\|_2$

Key observations:

- **Multiplicative noise does not scale with circuit depth.** In additive noise, every layer contributes equally to the error sum, so error grows with d. In multiplicative noise, each layer's contribution is weighted by $|\phi_j|$ (coherent) or ϕ_j^2 (stochastic). Phase factors decay rapidly away from the center of the QSP sequence, so the weighted sum is dominated by a small number of central layers and remains bounded as d grows.
- **First-order predictions hold across target functions and phase factor methods.** Empirical noisy behavior matches the analytic bounds for each noise model across diverse target functions (eigenstate filtering, Hamiltonian simulation, matrix inversion, Fermi-Dirac) and across phase factor methods (Prony, Newton, NLFT). The controlling quantities, $(d+1)|\varepsilon|$, $|\varepsilon||\mathrm{Re}\, S(x)|$, $\sigma\sqrt{d+1}$, $\sigma\|\Phi\|_2$, vary in magnitude across targets but consistently track observation.

Future Directions

- **Non-unitary noise.** Amplitude damping requires Lindbladian analysis; natural extension via process-tensor methods.
- **Algorithmic mitigation.** Develop algorithmic frameworks that use the error model as a feedback signal to make in-situ phase optimizations.

References

1. L. Ying, "Stable factorization for phase factors of quantum signal processing," *Quantum* **6**, 842 (2022).
2. A. K. Tan, Y. Liu, M. C. Tran, and I. L. Chuang, "Error Correction of Quantum Algorithms: Arbitrarily Accurate Recovery Of Noisy Quantum Signal Processing," arXiv:2301.08542 (2023).
3. S. Liu, Y. Dong, D. An, and M. Y. Niu, "Ensemble-Based Quantum Signal Processing for Error Mitigation," arXiv:2601.20073 (2026).
4. Dong, Y., Meng, X., Whaley, K.B. and Lin, L., 2021. Efficient phase-factor evaluation in quantum signal processing. Physical Review A, 103(4), p.042419.
5. Ni, H., Sarkar, R., Ying, L., & Lin, L. (2025). Inverse nonlinear fast Fourier transform on SU (2) with applications to quantum signal processing. arXiv preprint arXiv:2505.12615.